ARTICLE

A computational investigation into nickel-bis(diselenolene) complexes as potential catalysts for reduction of H⁺ to H₂

Briana T.A. Boychuk and Eric A.C. Bushnell

Abstract: As a result of burning fossil fuels, levels of greenhouse gases in our atmosphere are increasing at an alarming rate. Such an increase in greenhouse gases threatens our planet due to global climate change. To reduce the production of greenhouse gases, we must switch from fossil fuels to alternative fuels for energy. The most viable alternative energy source involves the conversion of solar energy into chemical energy via the photocatalytic splitting of water to form molecular hydrogen. In the present work, the Ni-bis(1,2-diamine-diselenolene) and Ni-bis(1,2-dicyano-diselenolene) complexes were studied using density functional theory (DFT). From the results, it was found that the 1,2-diamine-diselenolene and 1,2-dicyano-diselenolene nickel complexes catalyze the formation of $H_2(g)$ with overall reaction Gibbs energies of +8.7 kJ mol^{-1} and +8.4 kJ mol^{-1}, respectively, in a dilute aqueous environment versus the standard hydrogen electrode (SHE). Although both are able to catalyze the HER through a marginally endergonic reaction, the most thermodynamically favourable pathways differed between the complexes. In particular, the most thermodynamically favourable pathway for the formation of H_2 by ^{CN}Ox involves an EECC mechanism, whereas for ^{NH_2}Ox, the most thermodynamically favourable pathway occurs via an ECCE mechanism. From the results presented, the choice of substituent on the alkene backbone significantly affects the reduction potential and reaction Gibbs energies of protonation. The considerably more positive reduction potential for the CN complexes may offer a solution to the problems experimentally observed for the production of H_2.

Key words: hydrogen evolution reaction, HER catalysts, alternative fuels, diselenolene, density functional theory.

Résumé : À cause des niveaux de consommation des combustibles fossiles, la quantité de gaz à effet de serre dans l'atmosphère augmente à une vitesse alarmante. Une telle augmentation menace notre planète du fait qu'elle provoque des changements climatiques à l'échelle du globe. Afin de réduire la production de gaz à effet de serre, nous devons abandonner les combustibles fossiles et nous tourner vers des carburants de remplacement pour obtenir de l'énergie. La source d'énergie de remplacement la plus durable consiste à convertir l'énergie solaire en énergie chimique par dissociation photocatalytique de l'eau pour former de l'hydrogène moléculaire. Dans le cadre des présents travaux, nous avons étudié les complexes bis(1,2-diamine-disélénolène)nickel et bis(1,2-dicyano-disélénolène)nickel à l'aide de la théorie de la fonctionnelle de la densité (DFT). Selon nos résultats, nous avons découvert que les complexes de nickel de type 1,2-diamine-disélénolène et 1,2-dicyano-disélénolène catalysent la formation d'$H_2(g)$ avec une énergie de Gibbs de la réaction globale de +8,7 kJ mol^{-1} et de +8,4 kJ mol^{-1}, respectivement, dans un environnement aqueux dilué par rapport à l'électrode standard à hydrogène (ESH). Bien que les deux complexes aient été capables de catalyser la réaction à libération d'hydrogène par une réaction faiblement endergonique, la voie la plus favorable sur le plan thermodynamique n'était pas la même pour les deux complexes. À savoir, la voie la plus favorable sur le plan thermodynamique pour la formation d'H_2 par ^{CN}Ox fait intervenir un mécanisme de type EECC, tandis que la formation d'H_2 par ^{NH_2}Ox s'effectue préférentiellement par un mécanisme de type ECCE. D'après les résultats que nous présentons, le choix des substituants sur le squelette de l'alcène influe significativement sur le potentiel de réduction et sur les énergies de Gibbs de la protonation. Le fait que le potentiel de réduction des complexes CN soit considérablement plus positif pourrait constituer une solution aux problèmes de production d'H_2 que l'on observe expérimentalement. [Traduit par la Rédaction]

Mots-clés : réaction à libération d'hydrogène, catalyseurs de réactions à libération d'hydrogène, carburants de remplacement, disélénolène, théorie de la fonctionnelle de la densité.

Introduction

Increasing levels of greenhouse gases in our atmosphere threatens our planet as a result of climate change.[1] A main component of greenhouse gases is carbon dioxide and is a primary product of fossil-fuel consumption which is required for the planet's energy demands. In fact, 80% of the world's energy consumption is derived from the burning of fossil fuels.[2–5] Based on current emission levels of CO_2 into our atmosphere, the Earth is on track for continued global temperature increases. Importantly, it has been stated that an increase of 2 °C in Earth's mean temperature is considered a benchmark where the risk of climate change becomes threatening.[6] Based on the current levels of CO_2 emissions, the probability of reaching this 2 °C benchmark by 2100 is 88%![7] Thus, to prevent this increase of 2 °C, urgent action is required. Such action involves reduced fossil fuel consumption and the development of renewable energy sources to reduce the amount of CO_2 emitted into our atmosphere.[1,2,6–9]

As noted above, fossil fuels are a large contributor to carbon dioxide emissions; however, fossil fuels are a nonrenewable fuel source, thus regardless of environmental concerns, we must transition to renewable energy sources or risk running out of fossil

B.T.A. Boychuk and E.A.C. Bushnell. Department of Chemistry, Brandon University, 270 18th Street, Brandon, MB R7A 6A9, Canada.
Corresponding author: Eric A.C. Bushnell (email: bushnelle@brandonu.ca).

fuels.[6–9] Currently, there are several alternative energy sources available such as wind, solar, and tidal. The most viable path for large-scale growth of alternative energy sources involves solar energy conversion and, specifically, the photocatalytic splitting of water to form molecular hydrogen to be used as an alternative fuel.[2,10–12] Although hydrogen is the most abundant element in the universe, molecular hydrogen itself is not present on earth in significant amounts and must be produced from a hydrogen-containing source such as water. Electrolysis of water allows for conversion of electricity into chemical energy, allowing for separation of hydrogen from water. However, presently, there are limited methods available for hydrogen fuel production that are efficient and do so at relatively low costs. As a means to minimize costs, research is under way in the development of various catalysts using base metals such as copper, nickel, iron, and cobalt.[13] However, many catalysts investigated for the production of molecular hydrogen decompose over time due to the hydrogenation of the ligands.[14]

Of the various base-metal containing catalysts studied in the past, complexes containing dithiolene ligands showed favourable properties for the photocatalytic splitting of water to form hydrogen gas.[2,13,14] In particular, in the production of H$_2$ by dithiolene-containing catalysts, the unsaturated 1,2-dithiolene ligands are less susceptible to hydrogenation, which, as discussed above, resulted in the decomposition of previous catalysts.[13,15] Because metal–dithiolene complexes are capable of undergoing multi-electron processes, it has been proposed that the generation of hydrogen occurs through stepwise one-electron transfers and protonations.[2,15] The unique chemistry of dithiolene-containing complexes is a result of the noninnocent interaction between metal and ligands.[16] Dithiolene ligands are in fact prototypical redox-noninnocent ligands and undergo reversible redox reactions when coupled to a metal. An advantage of such redox-active ligands is that by varying the R groups attached to the ligand, properties of the complex can be tuned for a specific application.[13,15]

Analogous to the dithiolene ligands are the diselenolene ligands. Recent research has compared the chemistry of dithiolene- and diselenolene-containing complexes and has shown that both have very similar geometrical and chemical properties.[17–20] Although this past work has found that the nature of chalcogen atoms does not strongly affect the chemistry of such complexes, subtle differences do exist between dithiolene and diselenolene complexes. For instance, the diselenolene complexes are found to have a smaller HOMO–LUMO energy gap than analogous dithiolene complexes and are thus expected to have a slight increase in kinetic reactivity for electron transfer processes.[17,20]

Recently, for NiFe-hydrogenases, when the ligating cys was changed to sec–cys, an improvement in the hydrogen evolution reaction (HER) was observed as a result of changing the S atom to a Se atom.[21–24] This improvement was suggested to be due to the higher nucleophilicity of the selenocysteine and the lower pK_a of the –SeH moiety.[21–24] Similarly, experimental research has shown that in the case of Ni-bis(benzene-1,2,4,5-selenolate) polymers, replacement of S with Se reduces the overpotential needed for the HER. Moreover, the selenium catalysts showed significant improvement in durability of the catalysts under prolonged reductive acidic conditions.[25]

In the present work the 1,2-diamine-diselenolene and 1,2-dicyano-diselenolene nickel complexes were studied using density functional theory (DFT) calculations to investigate the HER of two Ni-bis(diselenolene) complexes. The choice of moieties attached to the ligands also allows the investigation into how an electron-donating or electron-withdrawing moiety affects the thermodynamics of reduction and protonation. The R-groups chosen included the strong electron-donating –NH$_2$ group, and the strong electron-withdrawing –CN group. The structures of the different nickel complexes studied are shown in Scheme 1.

Scheme 1. The oxidized structures of the cyano (^{CN}Ox) and amine (^{NH_2}Ox) containing Ni-bis(diselenolene) complexes investigated in the present work.
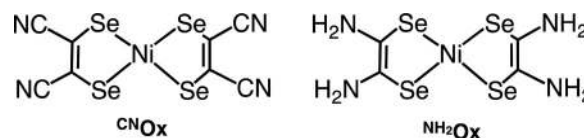
Methods

The Gaussian 09 software suite was used to perform all calculations. Geometry optimizations were performed at the B3LYP/6-31G(d) level of theory.[26–32] Single point energies were obtained at the IEFPCM-M06/6-311+G(2df,p) level of theory where the IEFPCM approach was used to model the presence of solvent on the reaction where water was chosen as the solvent.[33–39] Single-point energies were corrected to Gibbs energies by adding the Gibbs corrections calculated by performing frequency calculations at the B3LYP/6-31G(d) level of theory on the optimized geometries. The M06 functional was chosen due to past work, which has shown the accuracy of the functional when calculating reduction potentials of diselenolene complexes.[19,40,41] The M06 functional is a meta-hybrid functional for general-purpose applications and has been shown to be suitable for applications in transition metal chemistry giving better performance than B3LYP for main-group thermochemistry, barrier heights, and noncovalent interactions.[38,39]

We have considered the assembly of two protons and two electrons to form H$_2$ via a series of stepwise electron transfers and proton transfers. Using the Gibbs corrections and single-point energies, the relative reduction potentials (versus the standard hydrogen electrode (SHE)) (eqs. 1–3) and protonation energies in aqueous solution (eqs. 4 and 5) were obtained.

$$(1) \qquad [M(Se_2C_2R_2)_2]^z + e^- \rightarrow [M(Se_2C_2R_2)_2]^{z-1}$$

$$(2) \qquad \Delta_r G_s^o = \mu_{298k}^{0,g}(\text{RED}) + \Delta G_s^o(\text{RED}) - \mu_{298k}^{0,g}(\text{OX}) \\ - \Delta G_s^o(\text{OX}) - \mu_{298k}^{0,\text{SHE}}(e^-)$$

$$(3) \qquad E^o = \frac{-\Delta_r G_s^o}{F}$$

$$(4) \qquad [M(Se_2C_2R_2)_2]^z + H^+ \rightarrow [M(H)(Se_2C_2H_2)_2]^{z+1}$$

$$(5) \qquad \Delta_r G_s^o = \mu_{298k}^{0,g}(\text{acid}) + \Delta G_s^o(\text{acid}) - \mu_{298k}^{0,g}(\text{base}) \\ - \Delta G_s^o(\text{base}) - \mu_{298k}^{0,\text{aq}}(H^+)$$

where $\mu_{298k}^{0,g}(X)$ is the chemical potential in gas phase at 298 K for species X and $\Delta G_s^o(X)$ is the bulk energy of solvation. In accordance to the work by Llano and Eriksson,[42] the chemical potential of the electron ($\mu_{298k}^{0,\text{SHE}}(e^-)$) is –418.5 ± 2.1 kJ mol^{-1}, setting the calculated reduction potentials relative to the SHE, whereas the chemical potential of a proton in a dilute aqueous environment ($\mu_{298k}^{0,\text{aq}}(H^+)$) is –1124.2 ± 0.8 kJ mol^{-1}. The models used in the study are shown in Scheme 1.

Results and discussion

It has been previously been proposed that H$_2$ production by a series of Ni complexes occurs after two electrons and two protons have been added to the metal complex.[2] In particular, for a series of Ni—dithiolene complexes, Das et al.[2] proposed that an ECEC mechanism (E = electron transfer; C = chemical step) in the formation of H$_2$, where a ligand is first protonated followed by protonation of the Ni atom to form a metal–hydride.[2] For production of H$_2$ by metal selenloate polymers, Downes and Marinescu[25] pro-

Fig. 1. The Gibbs energies ($\Delta_r G_s^o$ in kJ mol^{-1}) and relative reduction potentials (E° in V) for the first electron transfer and protonation steps in the formation of H_2 by Ni-bis(diselenolene) complexes investigated herein. The reaction Gibbs energies and relative reduction potentials provided in terms of moiety attached to the alkene backbone is indicated by the CN or NH_2 in parentheses.
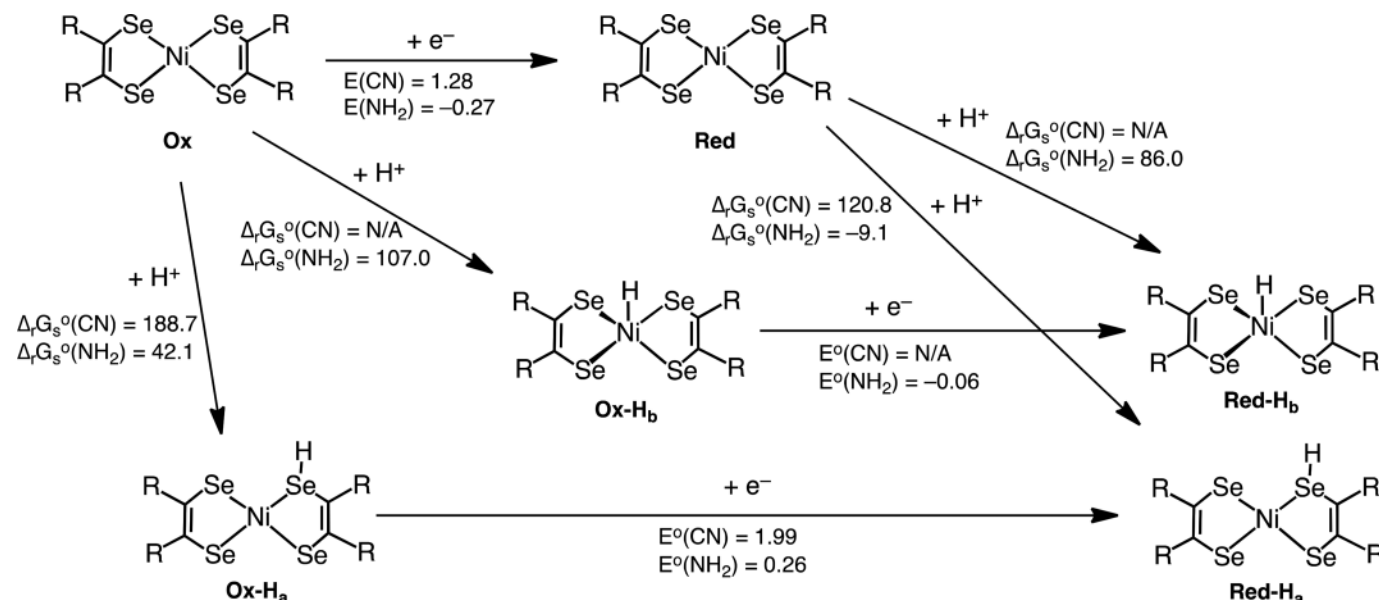
posed that, depending on the experimental conditions, two possible mechanisms exist for H_2 production. At more positive potentials, an ECCE mechanism is followed, whereas at more negative potentials, an ECEC mechanism is followed; however, no metal–hydride intermediate is proposed to exist in either mechanism.

In the present study, many possible mechanisms have been considered. The reaction Gibbs energies for protonation and relative the reduction potentials for the amine- and cyano-containing Ni-bis(diselenolene) complexes (Scheme 1) are provided in Figs. 1 and 2.

For the oxidized species ^{NH_2}Ox and ^{CN}Ox, two possible sites of protonation exist. The first site of protonation is a ligating selenium atom that leads to Ox–H$_a$, whereas the second protonation site is the central Ni atom and leads to Ox–H$_b$. From Fig. 1, the formation of Ox–H$_a$ in a dilute aqueous environment is endergonic for both the amine and cyano complexes, where addition of a proton to a selenium atom of ^{NH_2}Ox and ^{CN}Ox was found to occur with $\Delta_r G_s^o$ = 42.1 kJ mol^{-1} and $\Delta_r G_s^o$ = 188.7 kJ mol^{-1}, respectively. Therefore, in a dilute aqueous environment, protonation of either complex is thermodynamically unfavourable; however, it is noted that protonation of ^{NH_2}Ox is considerably less endergonic than the protonation of ^{CN}Ox ($\Delta\Delta_r G_s^o$ = 146.6 kJ mol^{-1}). Regarding the protonation of the Ni atom, it was found that the formation of ^{NH_2}Ox–H$_b$ is an endergonic process with a $\Delta_r G_s^o$ of 107.0 kJ mol^{-1} (Fig. 1). Due to the considerable cost in reaction Gibbs energy for protonation in a dilute aqueous environment, the protonation of the central Ni atom of ^{NH_2}Ox seems unlikely. Regarding ^{CN}Ox–H$_b$, at the B3LYP/6-31G(d) level of theory, the proton was found to migrate from the central Ni atom to a ligating Se atom. Thus, at the present level of theory, it appears that ^{CN}Ox–H$_b$ is not a stable intermediate. The preferential protonation of the ligand versus the central Ni atom supports the proposed mechanism of Das et al.,[2] as well as Downes and Marinescu,[25] where the first proton is added to the ligand.

Following the addition of a proton, the reduction potentials for the redox couples ^{CN}Ox–H$_a$/^{CN}Red–H$_a$ and ^{NH_2}Ox–H$_a$/^{NH_2}Red–H$_a$ were calculated to be 1.99 V and 0.26 V, respectively. Therefore, both redox couples are more oxidizing than the SHE. As stated above, a stable intermediate of the cyano derivative ^{CN}Red–H$_b$ could not be optimized at the present level of theory. In regard to the ^{NH_2}Ox–H$_b$/^{NH_2}Red–H$_b$ redox couple, the calculated reduction

potential is −0.06 V and is therefore marginally more reducing than the SHE.

If we consider the alternative of first reducing the oxidized species followed by protonation, the reduction potentials relative to the SHE for the ^{NH_2}Ox/^{NH_2}Red and ^{CN}Ox/^{CN}Red redox couples are calculated to be −0.27 V and +1.28 V (Fig. 1), respectively. Thus, relative to the SHE the reduction of the cyano-containing species is thermodynamically favourable whereas for the amine-containing complex reduction is not thermodynamically. Given the values in Fig. 1 the reduction of ^{NH_2}Ox and ^{CN}Ox is more likely than protonation at the present level of theory. Following the electron transfer, protonation of ^{NH_2}Red and ^{CN}Red can occur at a ligand Se atom or the central Ni atom. As stated above, the intermediate ^{CN}Red–H$_b$ did not exist at the present level of theory and therefore does not appear to be a stable intermediate in the formation of H_2. However, protonation of ^{NH_2}Red to form ^{NH_2}Red–H$_b$ occurs with a $\Delta_r G_s^o$ of 86.0 kJ mol^{-1} and therefore represents a considerable endergonic step in the formation of H_2. With the protonation of a ligating Se atom $\Delta_r G_s^o$ of 120.8 kJ mol^{-1} and −9.1 kJ mol^{-1} for ^{CN}Red and ^{NH_2}Red were calculated, respectively.

The reaction Gibbs energies and relative reduction potentials for the second protonation and second reduction are provided in Fig. 2, respectively. Note that Red–H$_b$ is not included in Fig. 2.

Due to the high energetic cost to protonate ^{CN}Red (Fig. 2), the possibility of a second reduction prior to protonation was considered; i.e., an EECC mechanism was considered. For purposes of completeness the possibility of a second reduction prior to formation of ^{NH_2}Red–H$_a$ was also considered. For the ^{CN}Red/^{CN}2Red and ^{NH_2}Red/^{NH_2}2Red redox couples, the relative reduction potentials are calculated to be 0.24 V and −0.69 V, respectively. Thus, relative to the SHE only, reduction of the ^{CN}Red/^{CN}2Red redox couples is thermodynamically favourable, whereas reduction of the ^{NH_2}Red/^{NH_2}Red redox couples is not. From Fig. 1, given that the protonation of ^{NH_2}Red in a dilute aqueous environment to form ^{NH_2}Red-H$_a$ occurs with a $\Delta_r G_s^o$ of −9.1 kJ mol^{-1}, it is unlikely that ^{NH_2}2Red represent a stable intermediate in the formation of H_2 in a dilute aqueous environment where the reducing electrons are coming from a SHE.

From Fig. 2, the reduction potential for the ^{NH_2}Red–H$_a$/^{NH_2}2Red–H$_a$ redox couple was calculated to be −0.50 V relative to the SHE and is therefore not a thermodynamically favourable process when

Fig. 2. The Gibbs energies ($\Delta_r G_s^o$ in kJ mol⁻¹) and relative reduction potentials (E° in V) for the second electron transfer and second protonation steps in the formation of H_2 by Ni-bis(diselenolene) complexes investigated herein. The reaction Gibbs energies and relative reduction potentials provided in terms of moiety attached to the alkene backbone is indicated by the CN or NH_2 in parentheses.
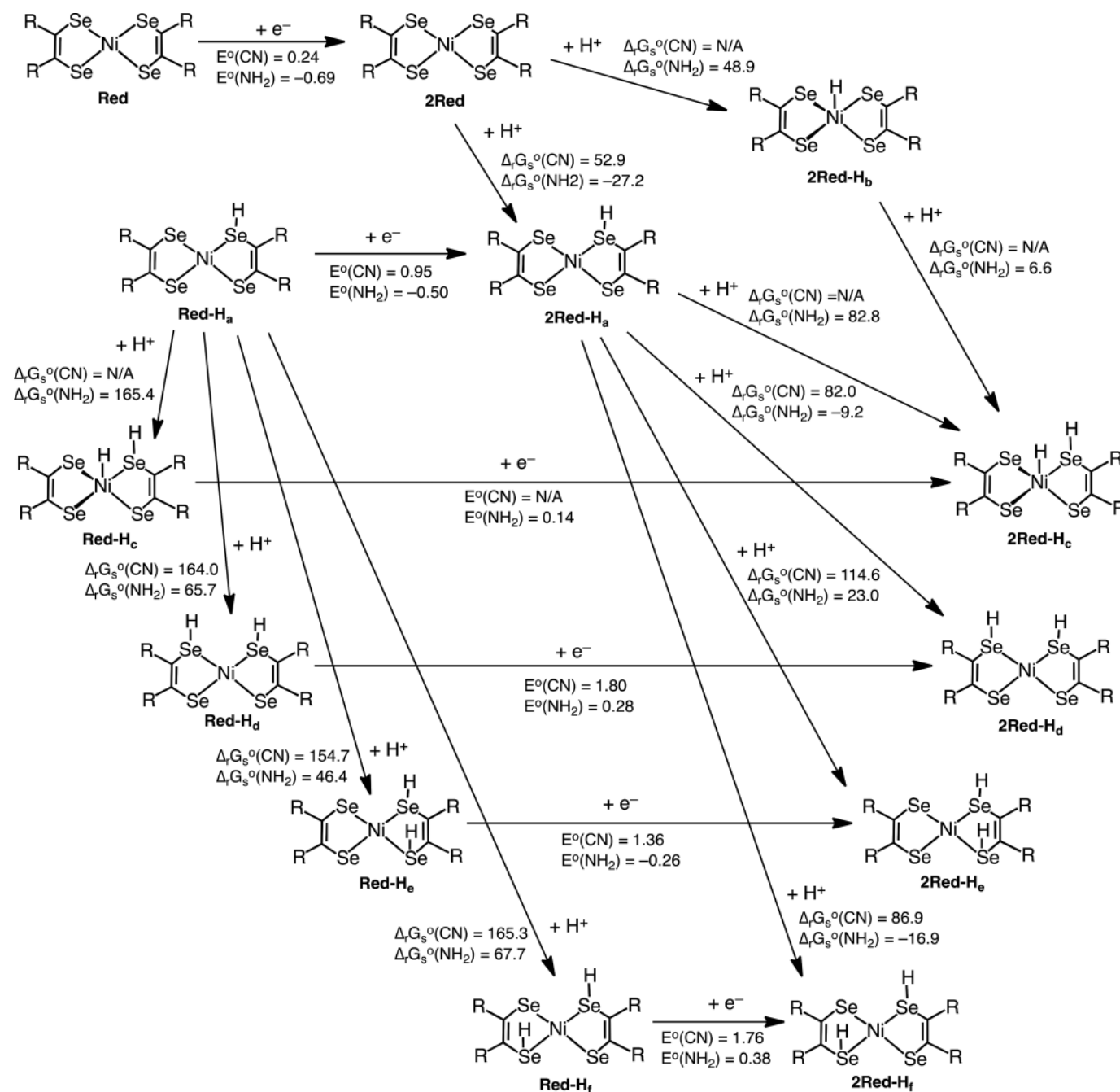

the reducing electrons are gained from the SHE. For the ^{CN}Red–H$_a$/^{CN}2Red–H$_a$ redox couple, a reduction potential of +0.95 V was calculated. However, given the considerable cost for formation of ^{CN}Red–H$_a$ (Fig. 2), it is unlikely that ^{CN}2Red–H$_a$ is formed.

Given the negative reduction potential of −0.50 V versus the SHE for the ^{NH_2}Red–H$_a$/^{NH_2}2Red–H$_a$ redox couple, the protonation of ^{NH_2}Red–H$_a$ was considered prior to a second reduction; i.e., an ECCE mechanism was considered. Regarding ^{NH_2}Red–H$_a$, four possible sites of protonation exist, for purposes of completeness, the CN derivative was also considered. As seen in Fig. 2, addition of a proton to the central nickel atom results in the formation of Red–H$_c$ and occurs with a $\Delta_r G_s^o$ of 252.1 kJ mol⁻¹ and 165.4 kJ mol⁻¹

for ^{CN}Red–H$_c$ and ^{NH_2}Red–H$_c$, respectively. Thus, given the considerable endergonicity for formation of ^{CN}Red–H$_c$ and ^{NH_2}Red–H$_c$, it is unlikely the formation of H_2 proceeds through such an intermediate. With the addition of the proton to the *cis* selenium atom on the adjacent diselenolene ligand forming ^{CN}Red–H$_d$ and ^{NH_2}Red–H$_d$, the $\Delta_r G_s^o$ was calculated to be 164.0 kJ mol⁻¹ and 65.7 kJ mol⁻¹, respectively. With the addition of a proton to the *cis* selenium atom, a doubly protonated diselenolene ligand occurs with $\Delta_r G_s^o$ of 154.7 kJ mol⁻¹ and 46.4 kJ mol⁻¹, resulting in the formation of ^{CN}Red–H$_e$ and ^{NH_2}Red–H$_e$, respectively. Lastly, protonation of the *trans* Se-atom $\Delta_r G_s^o$ of 165.3 kJ mol⁻¹ and 67.7 kJ mol⁻¹ were calculated for ^{CN}Red–H$_e$ and ^{NH_2}Red–H$_e$, respectively. Thus, given the

Fig. 3. The lowest energetic pathway for double protonation and double reduction of ^{CN}Ox forming ^{CN}2Red–H_d. The energies provided are strictly related to the thermodynamics of the reaction.
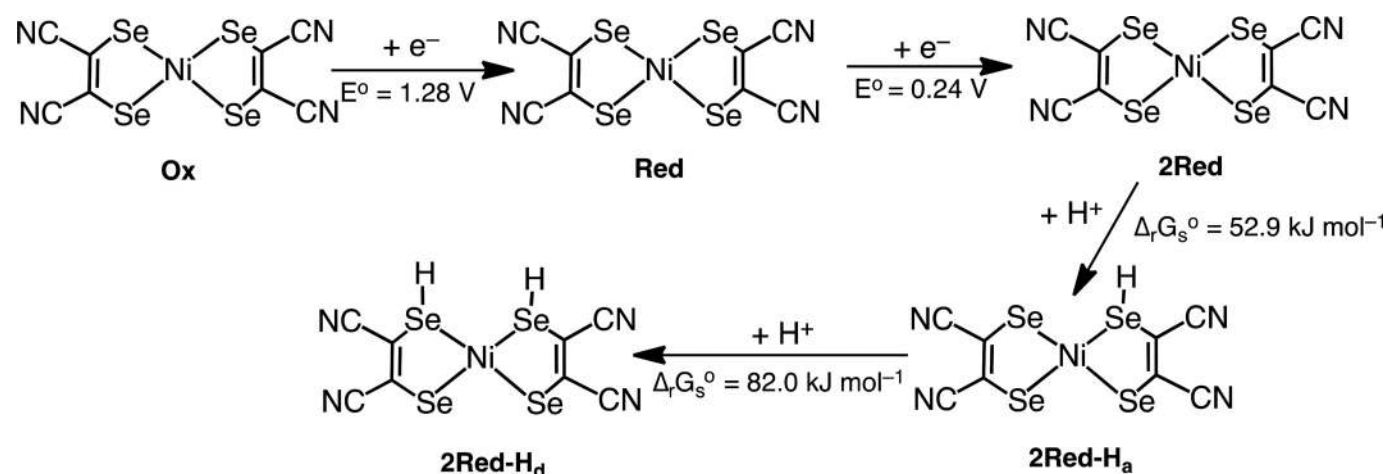
negative reduction potential of −0.50 V versus the SHE for the ^{NH_2}Red–H_a/^{NH_2}2Red–H_a redox couple in a dilute aqueous environment, the protonation of ^{NH_2}Red–H_a to form ^{NH_2}Red–H_e is marginally thermodynamically favoured, and therefore, ^{NH_2}Red–H_e is more favoured to form than ^{NH_2}2Red–H_a. With the formation of ^{NH_2}Red–H_e, reduction to ^{NH_2}2Red–H_e occurs at a relative reduction potential of −0.26 V. However, from **2**, given the very similar costs in Gibbs energy for formation of ^{NH_2}Red–H_e and ^{NH_2}2Red–H_a, the protonation of ^{NH_2}2Red–H_a to form ^{NH_2}2Red–H_d was considered. As seen in Fig. 2, this occurs as an exergonic process with a $\Delta_r G_s^o$ of −9.2 kJ mol^{-1}. Moreover, formation of ^{NH_2}2Red–H_f also occurs as an exergonic process with a $\Delta_r G_s^o$ of −16.9 kJ mol^{-1}. Although formation of ^{NH_2}Red–H_e is marginally more favourable than formation of ^{NH_2}2Red–H_a, it might be expected that under slightly reducing conditions in a dilute aqueous environment, ^{NH_2}2Red–H_a is likely first formed followed by protonation to form ^{NH_2}2Red–H_f. However, in acidic conditions, the reaction would most likely proceed through the formation of ^{NH_2}Red–H_e followed by reduction to form the complex, ^{NH_2}2Red–H_e. Regarding the CN derivative, the energies and reduction potentials provided in Figs. 1 and 2 suggest that the most likely pathway involves two one-electron reductions prior to protonation.

From Figs. 1 and 2, the lowest energetic pathway for double protonation and double reduction of ^{CN}Ox and ^{NH_2}Ox are shown in Figs. 3 and 4. Regarding ^{CN}Ox in a dilute aqueous environment versus the SHE, the pathway with the lowest energetic involves an EECC mechanism and results in the formation of ^{CN}2Red–H_d. From the energies provided in Fig. 3, the formation of ^{CN}2Red–H_d with an overall $\Delta_r G_s^o$ of −11.8 kJ mol^{-1}.

In the case of ^{NH_2}Ox in a dilute aqueous environment versus the SHE, the lowest energetic pathway involves an ECCE mechanism and results in the formation of 2Red–H_e with an overall $\Delta_r G_s^o$ of +88.4 kJ mol^{-1} (Fig. 4). Thus, at the IEFPCM-M06/6-311+G(2df,p)//B3LYP/6-31G(d) level of theory, the most thermodynamically favourable pathway for formation of H_2 in the presence of ^{NH_2}Ox and ^{CN}Ox occurs via an ECCE and EECC mechanism, respectively. As noted above, it has been proposed that generation of hydrogen occurs through stepwise electron transfers and protonations, because metal-dithiolene complexes are capable of undergoing multi-electron processes. The results presented herein support such a mechanism. Interestingly, in regards to the work by Downes and Marinescu,[25] it was proposed that for a series of Ni-bis(benzene-1,2,4,5-selenolate) polymers at more positive potentials, an ECCE mechanism is followed. At more negative potentials, ECEC mechanism occurs. As noted above, Das et al.[2] proposed that an ECEC mechanism in the formation of H_2 where

a ligand is first protonated followed by protonation of the Ni atom to form a metal–hydride.[2] The complex investigated by Das et al.[2] was the unsubstituted Ni-(bis(benzene-dithiolene), and therefore, the ligand would be slightly electron donating. From Figs. 1 and 2, only the amine-containing complex is able to form the Ni–H species at the present level of theory; however, due to the considerable energetic cost for the formation of ^{NH_2}2Red–H_c, it seems that, at the present level of theory, a Ni–H intermediate is unlikely to exist in the formation of H_2 in a dilute aqueous environment versus the SHE.

It is noted that in the work of Das et al., an issue with the Ni-bis(benzenedithiolene) was the need for very reducing conditions.[2] In the photocatalytic generation of H_2 from Ni-bis(benzenedithiolene), the reducing ability of the reduced fluorescein (Fl$^-$) to reduce the Ni complexes was insufficient for the production of H_2 gas.[2] From the values provided in Figs. 1 and 2, it is clear the choice of substituent on the alkene backbone both affects the reduction potential and reaction Gibbs energies of protonation. The ability of the moieties to affect the reduction potentials of diselenolene complexes has been previously investigated.[17,19,20,41] The considerably more positive reduction potential for the cyano complexes may offer a solution to the problems involved in the production of H_2, as seen by Das et al.[2]

With double reduction and double protonation, the last step in the mechanism is formation of H_2. For purposes of completeness the reaction Gibbs energies for the formation of H_2 from 2Red–H_d, 2Red–H_e, and 2Red–H_f are provided in Fig. 5. For the cyano complexes, the only doubly-reduced and doubly-protonated complex that results in the formation of H_2 via an exergonic step is ^{CN}2Red–H_e, whereas all amine-containing complexes undergo an exergonic process. Regarding the CN derivative, if we consider the most thermodynamically favourable pathway from Fig. 3, the formation of H_2 occurs with an overall $\Delta_r G_s^o$ of +8.7 kJ mol^{-1} and proceeds through ^{CN}2Red–H_d to reform ^{CN}Ox and H_2(g). Therefore, the formation of H_2 with the use of the CN-containing catalyst is marginally endergonic.

Similarly, if we consider the most thermodynamically favourable pathway from Fig. 4, the formation of H_2 likely passes through the intermediate ^{NH_2}2Red–H_e and occurs with an overall $\Delta_r G_s^o$ of +8.4 kJ mol^{-1}. Therefore, the overall Gibbs energy for the formation of H_2 is essentially identical regardless of the choice of moiety attached to the alkene backbone of the diselenolene ligand; however, the thermodynamics of each individual step differs greatly depending on moiety chosen. In particular, from the results presented, the choice of the cyano moieties results in complexes that are more oxidizing but more difficult to protonate,

Fig. 4. The lowest energetic pathway for double protonation and double reduction of ^{NH_2}Ox forming $^{NH_2}2Red–H_d$. The energies provided are strictly related to the thermodynamics of the reaction.
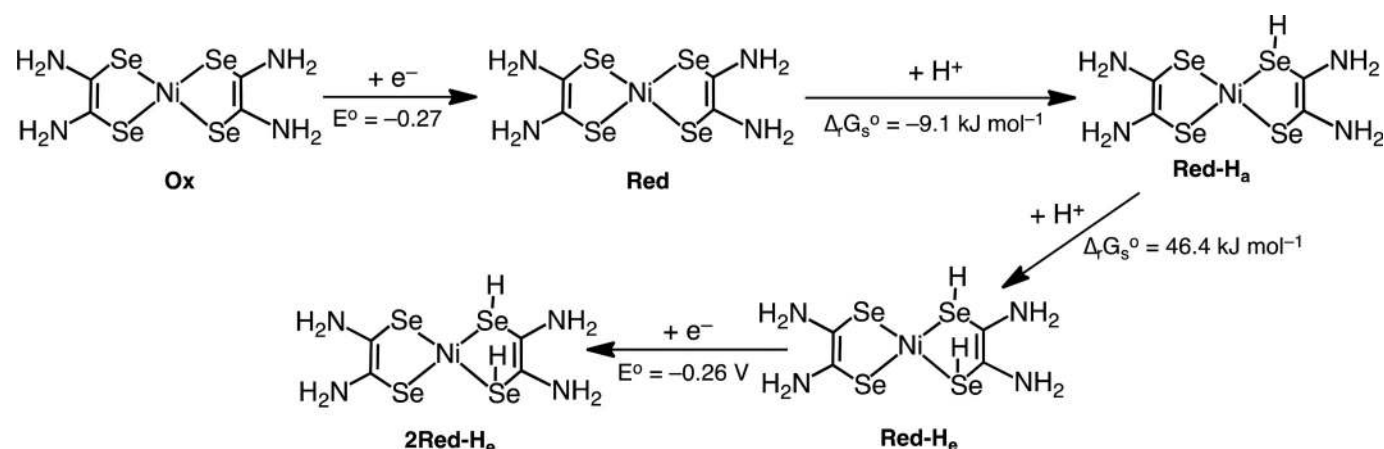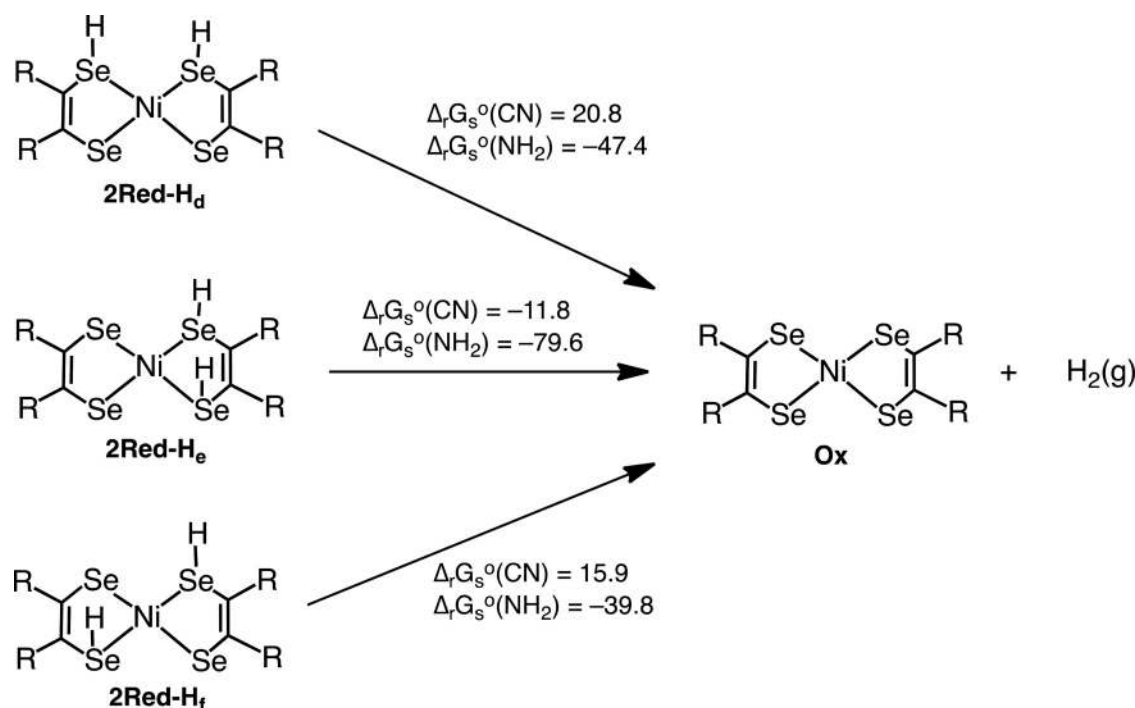

Fig. 5. The Gibbs energies ($\Delta_rG_s^o$ in kJ mol^{-1}) for the formation of $H_2(g)$ by Ni-bis(diselenolene) complexes. The reaction Gibbs energies provided are given in terms of moiety attached to the alkene backbone of the diselenolene ligand where the moiety is indicated by R = CN or NH_2.

whereas the choice of amine moieties results in compounds that are reducing compared with the SHE yet thermodynamically favourable to being protonated in a dilute aqueous environment.

Conclusion

In the present manuscript, the thermodynamics for the production of H_2 by ^{CN}Ox and ^{NH_2}Ox was investigated. In particular, the thermodynamics for many reactions involving sequential one-electron reductions or protonation steps were investigated. From the results obtained at the IEFPCM-M06/6-311+G(2df,p)//B3LYP/6-31G(d) level of theory, it was found that both the ^{CN}Ox and ^{NH_2}Ox catalyze the formation of $H_2(g)$ with overall $\Delta_rG_s^o$ of +8.7 kJ mol^{-1} and +8.4 kJ mol^{-1}, respectively, in a dilute aqueous environment versus the SHE. Thus, both catalysts catalyze the formation of H_2 via a marginally endergonic pathway. However, in regards to ^{CN}Ox, the most thermodynamically favourable pathway involves an EECC mechanism, whereas in the case of ^{NH_2}Ox, the most

thermodynamically favourable pathway occurs via an ECCE mechanism. From the results presented, the choice of substituent on the alkene backbone considerably affects thermodynamics of the individual steps. Importantly, the considerably more positive reduction potential for the CN complexes may offer a solution to the problems involved in the production of H_2 seen in past experimental work.

Supplementary data

The xyz coordinates of the complexes discussed in the present article are provided in Supplementary Table S1. Supplementary data are available with the article through the journal Web site at http://nrcresearchpress.com/doi/suppl/10.1139/cjc-2017-0565.

Acknowledgements

WESTGRID, SHARCNET, and Compute Canada for computational resources.

References

(1) Peters, G. P.; Andrew, R. M.; Boden, T.; Canadell, J. G.; Ciais, P.; Le Quéré, C.; Marland, G.; Raupach, M. R.; Wilson, C. *Nat. Clim. Change* **2013**, *3*, 4. doi:10.1038/nclimate1783.

(2) Das, A.; Han, Z.; Brennessel, W. W.; Holland, P. L.; Eisenberg, R. *ACS Catal.* **2015**, *5*, 1397. doi:10.1021/acscatal.5b00045.

(3) U.S. Department of Energy, Energy Information Administration, Annual Energy Outlook 2013 with Projections to 2040, Washington, DC, 2013, p. 55–90.

(4) U.S. Department of Energy, Energy Information Administration, International Energy Outlook 2013 with Projections to 2040, Washington, DC, 2013, p. 1–22.

(5) Hoffert, M. I.; Caldeira, K.; Jain, A. K.; Haites, E. F.; Harvey, L. D. D.; Potter, S. D.; Schlesinger, M. E.; Schneider, S. H.; Watts, R. G.; Wigley, T. M. L.; Wuebbles, D. J. *Nature* **1998**, *395*, 881. doi:10.1038/27638.

(6) Sottong, J.; Broomfield, M.; MacCarthy, J.; Misra, A.; Thistlethwaite, G.; Watterson, J. In *Still Only One Earth: Progress in the 40 Years Since the First UN Conference on the Environment*; Harrison, R. M., Hester, R. E., Eds.; The Royal Society of Chemistry: Cambridge, 2015; p. 34. doi:10.1039/9781782622178-00034.

(7) Capellán-Pérez, I.; Arto, I.; Polanco-Martínez, J. M.; González-Eguino, M.; Neumann, M. B. *Energy Environ. Sci.* **2016**, *9*, 2482. doi:10.1039/C6EE01008C.

(8) Kahn, B. We Just Breached the 410 PPM Threshold for CO_2. Available from www.scientificamerican.com/article/we-just-breached-the-410-ppm-threshold-for-co2/.

(9) Jakob, M.; Hilaire, J. *Nature* **2015**, *517*, 150. doi:10.1038/517150a.

(10) Alstrum-Acevedo, J. H.; Brennaman, M. K.; Meyer, T. J. *Inorg. Chem.* **2005**, *44*, 6802. doi:10.1021/ic050904r.

(11) Bard, A. J.; Fox, M. A. *Acc. Chem. Res.* **1995**, *28*, 141. doi:10.1021/ar00051a007.

(12) Lewis, N. S.; Nocera, D. G. *Proc. Natl. Acad. Sci. U.S.A.* **2006**, *103*, 15729. doi:10.1073/pnas.0603395103.

(13) Zarkadoulas, A.; Field, M. J.; Papatriantafyllopoulou, C.; Fize, J.; Artero, V.; Mitsopoulou, C. A. *Inorg. Chem.* **2016**, *55*, 432. doi:10.1021/acs.inorgchem.5b02000.

(14) McNamara, W. R.; Han, Z.; Yin, C.-J.; Brennessel, W. W.; Holland, P. L.; Eisenberg, R. *Proc. Natl. Acad. Sci. U.S.A.* **2012**, *109*, 15594. doi:10.1073/pnas.1120757109.

(15) Eisenberg, R.; Gray, H. B. *Inorg. Chem.* **2011**, *50*, 9741. doi:10.1021/ic2011748.

(16) Davison, A.; Edelstein, N.; Holm, R. H.; Maki, A. H. *J. Am. Chem. Soc.* **1964**, *86*, 2799. doi:10.1021/ja01068a010.

(17) Bushnell, E. A. C.; Adams, M. R.; Boyd, R. J. *Struct. Chem.* **2017**, *28*, 1173. doi:10.1007/s11224-017-0926-y.

(18) Bushnell, E. A. C. *Can. J. Chem.* **2016**, *94*, 1127. doi:10.1139/cjc-2016-0244.

(19) Bushnell, E. A. C.; Boyd, R. J. *J. Phys. Chem. A* **2015**, *119*, 911. doi:10.1021/jp511350z.

(20) Bushnell, E. A. C.; Boyd, R. J. *Int. J. Quantum Chem.* **2016**, *116*, 369. doi:10.1002/qua.25044.

(21) Wombwell, C.; Caputo, C. A.; Reisner, E. *Acc. Chem. Res.* **2015**, *48*, 2858. doi:10.1021/acs.accounts.5b00326.

(22) Figliola, C.; Male, L.; Horton, P. N.; Pitak, M. B.; Coles, S. J.; Horswell, S. L.; Grainger, R. S. *Organometallics* **2014**, *33*, 4449. doi:10.1021/om500683p.

(23) Wombwell, C.; Reisner, E. *Dalton Trans.* **2014**, *43*, 4483. doi:10.1039/C3DT52967C.

(24) Wombwell, C.; Reisner, E. *Chem. - Eur. J.* **2015**, *21*, 8096. doi:10.1002/chem.201500311.

(25) Downes, C. A.; Marinescu, S. C. *ACS Catal.* **2017**, *7*, 848. doi:10.1021/acscatal.6b03161.

(26) Becke, A. D. *J. Chem. Phys.* **1993**, *98*, 1372. doi:10.1063/1.464304.

(27) Becke, A. D. *J. Chem. Phys.* **1993**, *98*, 5648. doi:10.1063/1.464913.

(28) Handy, N. C.; Cohen, A. J. *Mol. Phys.* **2001**, *99*, 403. doi:10.1080/00268970010018431.

(29) Lee, C.; Yang, W.; Parr, R. G. *Phys. Rev. B* **1988**, *37*, 785. doi:10.1103/PhysRevB.37.785.

(30) Stephens, P. J.; Devlin, F. J.; Chabalowski, C. F.; Frisch, M. J. *J. Phys. Chem.* **1994**, *98*, 11623. doi:10.1021/j100096a001.

(31) Vosko, S. H.; Wilk, L.; Nusair, M. *Can. J. Phys.* **1980**, *58*, 1200. doi:10.1139/p80-159.

(32) Frisch, M. J.; Trucks, G. W.; Schlegel, H. B.; Scuseria, G. E.; Robb, M. A.; Cheeseman, J. R.; Scalmani, G.; Barone, V.; Mennucci, B.; Petersson, G. A.; Nakatsuji, H.; Caricato, M.; Li, X.; Hratchian, H. P.; Izmaylov, A. F.; Bloino, J.; Zheng, G.; Sonnenberg, J. L.; Hada, M.; Ehara, M.; Toyota, K.; Fukuda, R.; Hasegawa, J.; Ishida, M.; Nakajima, T.; Honda, Y.; Kitao, O.; Nakai, H.; Vreven, T.; Montgomery, J. A., Jr.; Peralta, J. E.; Ogliaro, F.; Bearpark, M.; Heyd, J. J.; Brothers, E.; Kudin, K. N.; Staroverov, V. N.; Keith, T.; Kobayashi, R.; Normand, J.; Raghavachari, K.; Rendell, A.; Burant, J. C.; Iyengar, S. S.; Tomasi, J.; Cossi, M.; Rega, N.; Millam, J. M.; Klene, M.; Knox, J. E.; Cross, J. B.; Bakken, V.; Adamo, C.; Jaramillo, J.; Gomperts, R.; Stratmann, R. E.; Yazyev, O.; Austin, A. J.; Cammi, R.; Pomelli, C.; Ochterski, J. W.; Martin, R. L.; Morokuma, K.; Zakrzewski, V. G.; Voth, G. A.; Salvador, P.; Dannenberg, J. J.; Dapprich, S.; Daniels, A. D.; Farkas, O.; Foresman, J. B.; Ortiz, J. V.; Cioslowski, J.; Fox, D. J. *Gaussian 09, Revision D.01*; Gaussian, Inc.: Wallingford, CT, 2010.

(33) Cancès, E.; Mennucci, B.; Tomasi, J. *J. Chem. Phys.* **1997**, *107*, 3032. doi:10.1063/1.474659.

(34) Mennucci, B.; Cancès, E.; Tomasi, J. *J. Phys. Chem. B* **1997**, *101*, 10506. doi:10.1021/jp971959k.

(35) Mennucci, B.; Tomasi, J. *J. Chem. Phys.* **1997**, *106*, 5151. doi:10.1063/1.473558.

(36) Tomasi, J.; Mennucci, B.; Cammi, R. *Chem. Rev.* **2005**, *105*, 2999. doi:10.1021/cr9904009.

(37) Tomasi, J.; Mennucci, B.; Cancès, E. *J. Mol. Struct.: THEOCHEM* **1999**, *464*, 211. doi:10.1016/S0166-1280(98)00553-3.

(38) Zhao, Y.; Truhlar, D. G. *Acc. Chem. Res.* **2008**, *41*, 157. doi:10.1021/ar700111a.

(39) Zhao, Y.; Truhlar, D. G. *Theor. Chem. Acc.* **2008**, *120*, 215. doi:10.1007/s00214-007-0310-x.

(40) Bushnell, E. A. C.; Burns, T. D.; Boyd, R. J. *J. Chem. Phys.* **2014**, *140*, 18A519. doi:10.1063/1.4867537.

(41) Bushnell, E. A. C.; Burns, T. D.; Boyd, R. J. *Phys. Chem. Chem. Phys.* **2014**, *16*, 10897. doi:10.1039/c4cp01105h.

(42) Llano, J.; Eriksson, L. A. *J. Chem. Phys.* **2002**, *117*, 10193. doi:10.1063/1.1516786.